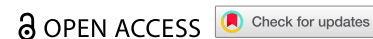


SHORT COMMUNICATION



The nuclear dynamic of CDC48 is affected during the immune response in plants

Damien Inès^a, Aymeric Leray^b, Pascale Winckler^c, Pierre-Emmanuel Courty^a, David Wendehenne^a, and Claire Rosnoblet^a

^aUniversité Bourgogne Europe, Institut Agro Dijon, INRAE, UMR Agroécologie, Dijon, France; ^bLaboratoire Interdisciplinaire Carnot de Bourgogne CNRS UMR 6303, Université Bourgogne Europe, Dijon, France; ^cDimacell Imaging Facility, L'Institut Agro Dijon, INRAE, INSERM, Université Bourgogne Europe, Université Marie & Louis Pasteur, Dijon, France

ABSTRACT

Plants are continuously challenged by a myriad of pathogenic microorganisms, including bacteria, viruses, fungi and oomycetes, against which they must defend themselves. The protein Cell Division Cycle 48 (CDC48), a key player of ubiquitin-proteasome system which segregates and remodels ubiquitinated proteins for degradation, is known to be mobilized during plant immunity. Moreover, the characterization of the nuclear role of CDC48 is of interest, in particular its regulation in nuclear processes such as chromatin remodeling, DNA repair and gene expression. In this regard, its nuclear functions during plant immunity remain underexplored. This study investigates the dynamics of CDC48 during plant immune responses. The biophysical analysis using the Fluorescence Correlation Spectroscopy (FCS) on tobacco leaves stably overexpressing GFP-CDC48 revealed that the nuclear dynamics of CDC48 changed after treatment with cryptogeiin, an elicitor of immune responses. FCS analysis revealed an increase of the nuclear mobility of CDC48 and a faster interaction of CDC48 with a wide range of nuclear partners shortly after cryptogeiin treatment. Overall, our study shows a nuclear regulation of the interaction of CDC48 with its potential partners and sheds new light on potential nuclear involvements of CDC48 following the triggering of defense mechanisms.

ARTICLE HISTORY

Received 7 February 2025
Revised 26 March 2025
Accepted 29 March 2025

KEYWORDS

Cell division cycle 48; plant immunity; biophysics; fluorescence correlation spectroscopy; cryptogeiin

Introduction

In their environment, plants are exposed to various microorganisms, some of which being pathogenic (bacteria, viruses, fungi). As a result, they set up defensive reactions which are finely regulated.¹ Studies have estimated that the expression of up to 20% of plant genes were significantly modified during plant immune responses.^{1,2} These regulated genes are involved in plant defense and encode for a myriad of proteins with various functions, including antimicrobial proteins and enzymes involved in the biosynthesis of metabolites.^{1,3,4} This large-scale and tightly transcriptional reprogramming can lead to a strengthening of the plant cell wall and, in some cases, trigger a localized cell death response (hypersensitive response) limiting the spread of pathogens.^{4–6} Several proteins related to the regulation of protein homeostasis, including Cell Division Cycle 48 (CDC48), are involved in plant immune response. CDC48 is an ATPase chaperone-like protein highly conserved protein across plants, yeast and mammals (known as Valosin Containing Protein, VCP, in mammals, or p97 in all organisms). CDC48 segregates ubiquitinated proteins from protein complexes and subcellular structures, such as membranes or chromatin, then remodels and sends them to the proteasome for degradation.⁷ Consequently, CDC48 is essential for protein quality control through the Ubiquitin Proteasome System (UPS). Additionally, it regulates diverse nuclear

functions, such as cell cycle, DNA repair, chromatin remodeling, inner nuclear membrane protein associated degradation (INMAD) and gene expression^{8–15}; Figure 1). In particular, CDC48 plays an essential role in the assembly and disassembly of protein – DNA complexes and in degradation of misfolded nuclear proteins.^{16,17} For example, CDC48 regulates transcription by segregating the polyubiquitinated transcriptional repressor alpha2 before sending it to degradation.¹⁵ More recently, CDC48 has been shown to regulate nuclear morphology through INMAD-mediated degradation of the SUN protein.⁸

CDC48 is known to be mobilized during plant immunity. For instance, CDC48 has been shown to specifically accumulate in cells in response to cryptogeiin, an elicitor produced by the oomycete *Phytophthora cryptogea* that triggers an immune response in tobacco. Moreover, cryptogeiin treatment in CDC48-overexpressing stable cell lines has been linked to premature HR-like cell death.^{18,19} CDC48 is also involved in the turnover of immune receptors and pathogenesis effectors.²⁰ Furthermore, following tobacco mosaic virus infection, no necrosis was observed in leaves of tobacco plants overexpressing CDC48,²¹ highlighting its role in virus resistance. Nevertheless, while CDC48 is recognized as a new player in plant immune responses, its nuclear role has not yet been characterized. Our targeted study aims to characterize the nuclear dynamics of CDC48 during the plant immune response.

CONTACT Claire Rosnoblet ✉ claire.rosnoblet@ube.fr Université Bourgogne Europe, Institut Agro Dijon, INRAE, UMR Agroécologie, 17 rue Sully, Dijon cedex 21065, France

© 2025 The Author(s). Published with license by Taylor & Francis Group, LLC.

This is an Open Access article distributed under the terms of the Creative Commons Attribution License (<http://creativecommons.org/licenses/by/4.0/>), which permits unrestricted use, distribution, and reproduction in any medium, provided the original work is properly cited. The terms on which this article has been published allow the posting of the Accepted Manuscript in a repository by the author(s) or with their consent.

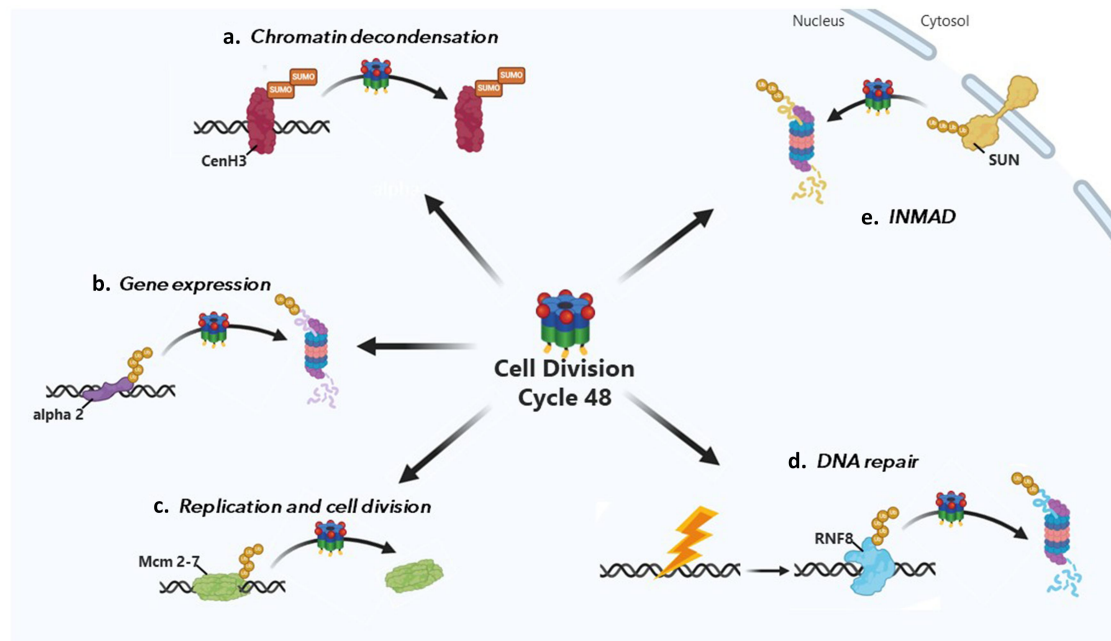


Figure 1. Nuclear functions of CDC48. (a) Chromatin Decondensation Regulation. In *Arabidopsis*, CDC48 interacts with sumoylated cenH3 to segregate it from chromatin, decondensing DNA regions required for ribosomal RNA synthesis, thereby promoting pollen tube growth.¹¹ (b) Regulation of gene expression. CDC48 facilitates transcription by segregating the polyubiquitinated alpha2 transcriptional repressor and degrading it via the proteasome.¹⁵ (c) Replication and cell division regulation. CDC48 halts DNA replication by extracting ubiquitinated CMG helicase complexes through the recognition and segregation of the Mcm7 subunit.⁹ (d) DNA repair regulation. Following DNA damage repair, CDC48 segregates and targets to the proteasomal degradation the ubiquitin ligase RNF8.¹³ (e) INMAD. CDC48 plays a crucial role in the degradation of inner nuclear membrane proteins (INMAD), including SUN proteins, which are key regulators of nuclear morphology.⁸

Materials and methods

Treatments and chemicals

Nicotiana tabacum cv. Xanthi plants stably overexpressing GFP-CDC48 (green fluorescent protein tag at the N-terminal part of CDC48,^{18,21} were grown at 24°C, 16 h day/8 h night. Cryptogein was purified according to Bonnet et al.²² and stored at −20°C as a 100 μM stock aqueous solution. Tobacco leaves were infiltrated either with water or with cryptogein (final concentration of 100 nM) using a syringe. All the experiments were performed on three independent biological replicates.

Fluorescence correlation spectroscopy (FCS)

FCS analysis were performed on the fourth leaf of two-month-old tobacco plants overexpressing GFP-CDC48, 30 minutes after water or cryptogein infiltration. GFP-CDC48 overexpressors exhibit approximately twice the endogenous level of CDC48.²¹ FCS measurements were conducted on a Nikon A1-MP two photon scanning microscope (Nikon, Japan) with a ×60 Apo IR objective (NA: 1.27, Water Immersion, Nikon). A 880 nm laser (Chameleon Vision II, Coherent) provided the excitation light. Fluorescence emission of GFP was collected through a band-pass emission filter FF01–520/35 (Semrock), using a Single-Photon Avalanche Diode detector connected to a Picoquant single photon counting module (Picoquant, Germany). Measurements were performed at room temperature (22°C) on cell nucleus. Each FCS measurement was recorded during

120 s to obtain a sufficient ACF accuracy. Each point represents the mean of three measurements per nucleus. Fifteen nuclei were recorded per experimental condition. Fluorescence time traces were analyzed with EasyFCS, a home-made software (free of charge: <https://github.com/ayleray/EasyFCS>.) written in MATLAB (version R2023B; The MathWorks, Natick, MA) that calculates the autocorrelation function (ACF also noted $G(\tau)$) with the time-tag-to-correlation algorithm developed by Wahl et al.²³ EasyFCS was also used for filtering the ACF and reducing the auto-fluorescence (fluorescence lifetime) by separating the intrinsic fluorescence from the scattered light.²⁴ A moving average detrending with a sliding window of 3 s was finally applied in EasyFCS to remove the slow intensity variations due to cell movements.

To estimate the association and dissociation rates at immobile binding sites within live cells, we have fitted these pre-processed ACFs with the full model for diffusion and binding developed by Michelman-Ribeiro et al.²⁵:

$$G(\tau) = \frac{w_0^2 z_0}{8N(2\pi)^{3/2}} \iint \frac{(1 - \phi)e^{-\frac{k_1\tau}{2}} + (1 + \phi)e^{-\frac{k_2\tau}{2}}}{2} \left(e^{-\frac{w_0^2}{4}q_r^2 - \frac{z_0^2}{4}q_z^2} \right) 2\pi q_r dq_r dq_z$$

Where N is the number of molecules in the observation volume, w_0 and z_0 are the lateral and axial extents of the Gaussian beam defined as the distances where the intensity is

reduced by a factor $1/\epsilon^2$, and q_r and q_z are the lateral and axial Fourier transform variables, respectively.

ϕ , k_1 and k_2 values are given by:

$$\phi = \frac{(k_{on}^* + k_{off})^2 + (k_{on}^* - k_{off})(q_r^2 + q_z^2)D}{(k_{on}^* + k_{off})\sqrt{(D(q_r^2 + q_z^2) + k_{on}^* + k_{off})^2 - 4D(q_r^2 + q_z^2)k_{off}}}$$

$$k_1 = \frac{D(q_r^2 + q_z^2) + k_{on}^* + k_{off}}{\sqrt{(D(q_r^2 + q_z^2) + k_{on}^* + k_{off})^2 - 4D(q_r^2 + q_z^2)k_{off}}}$$

$$k_2 = \frac{D(q_r^2 + q_z^2) + k_{on}^* + k_{off}}{-\sqrt{(D(q_r^2 + q_z^2) + k_{on}^* + k_{off})^2 - 4D(q_r^2 + q_z^2)k_{off}}}$$

Where D is the diffusion coefficient and k_{on}^* and k_{off} are the association and dissociation binding rates to an immobile substrate (in s^{-1}).

We have then calculated four parameters: the number of molecules in the observation volume N , the diffusion coefficient D , and the association and dissociation rates (k_{on}^* and k_{off}). We used the trust-region-reflective least squares algorithm to minimize the sum of the squared error between the experimental data and the full model. To retrieve the value of the association rate k_{on} in $M^{-1}s^{-1}$, we have divided k_{on}^* by the concentration c :

$$k_{on} = \frac{k_{on}^*}{c} = k_{on}^* \frac{\pi^{3/2} N_A w_0^2 z_0}{2^{3/2} N}$$

With N_A , the Avogadro constant. The dimensions of the observation volume (w_0 and z_0) were fixed to $w_0 = 0.22 \mu m$ and $z_0 = 0.6 \mu m$ after calibration with a 10 nM concentration solution of Atto 488 in water whose diffusion coefficient at 37° is $540 \mu m^2/s$ (ref: Peter Kapusta, PicoQuant GmbH Application Note, 2010 https://www.picoquant.com/images/uploads/page/files/7353/appnote_diffusioncoefficients.pdf).

Results

A biophysical analysis was performed using Fluorescence Correlation Spectroscopy (FCS) to characterize the nuclear

dynamics of CDC48 during the early events of the plant immune response triggered by cryptogin. FCS analyses were performed on tobacco leaves stably expressing GFP-CDC48, 30 minutes after water or cryptogin infiltration. The association/dissociation (Kon/Koff) model was chosen to provide insights into CDC48 nuclear dynamics through three parameters: the diffusion coefficient (D , in $\mu m^2 s^{-1}$) is related to the mobility of CDC48 across a defined area; the rate of association (Kon, in $M^{-1} s^{-1}$) reflects the interaction binding speed and the number of CDC48 partners; the dissociation rate (Koff, in s^{-1}) among CDC48 and its partners. We also calculated the dissociation constant $K_d = Koff/Kon$ (in M) to characterize the binding affinity. FCS is a reliable and efficient technique for determining the cellular dynamics of a protein.²⁶ This technique has already been used in plants to study the dynamics of membrane proteins within the cell.^{27–29}

The number of GFP-CDC48 molecules was significantly reduced within the studied nuclear volume, from about 48 to 32 molecules, when comparing leaves infiltrated with water and with cryptogin (Figure 2a). The diffusion coefficient (D) and the association rate (Kon) of CDC48 in tobacco leaves significantly increased after cryptogin infiltration, from $3.5 \mu m^2.s^{-1}$ to $8.4 \mu m^2.s^{-1}$ and from $3.5 \mu M^{-1}.s^{-1}$ to $14.1 \mu M^{-1}.s^{-1}$, respectively (Figure 2b and c). In contrast, the dissociation rate (Koff) remains constant in leaves infiltrated with water or with cryptogin, of about $35 s^{-1}$ (Figure 2d). The k_d value significantly decreased under cryptogin treatment, from 8.1 to $2.4 \mu M$, suggesting an increase of the binding affinity of CDC48 for its partners (Figure 2e).

Discussion

In our study, the diffusion coefficient (D) of CDC48 in tobacco leaves infiltrated with water was about $3.5 \mu m^2.s^{-1}$. Our results are similar to those of Aker et al.²⁷ reporting a FCS analysis of CDC48, suggesting an accurate calibration of the measured parameters. D increased significantly in tobacco leaves infiltrated with cryptogin to $8.4 \mu m^2.s^{-1}$, suggesting that free CDC48 (not bound to partners) is more mobile within the nucleus in the early stages of the immune response. At the same time, we measured

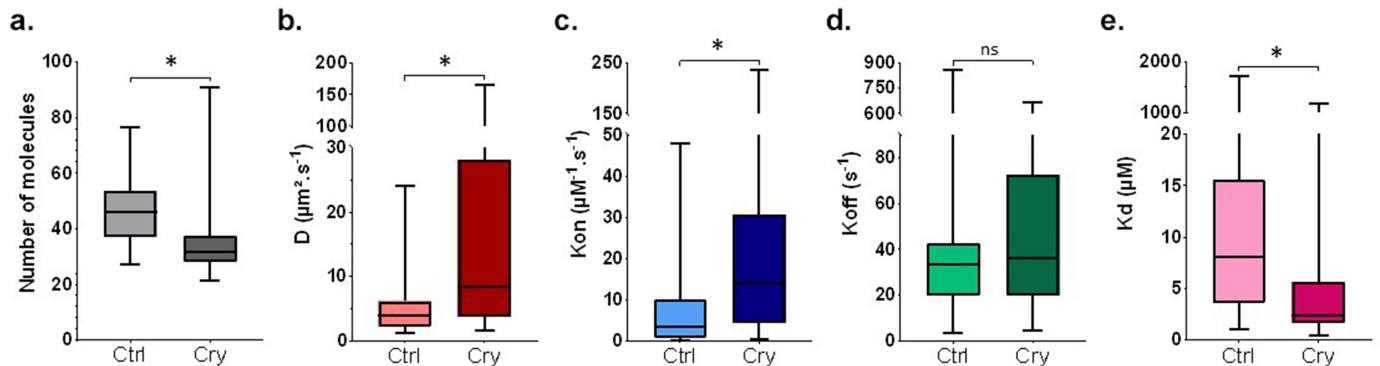


Figure 2. Biophysical analysis of CDC48 nuclear dynamics, using the FCS technique, 30 minutes after the treatment with cryptogin. (a) Number of molecules of GFP-CDC48 within the analyzed volume. (b) Diffusion coefficient of CDC48 (D , $\mu m^2.s^{-1}$). (c) Association rate of CDC48 with its partners (Kon, $\mu M^{-1}.s^{-1}$). (d) Dissociation rate of CDC48 with its partners (Koff, s^{-1}). (e) Dissociation constant of CDC48 with its partners (K_d , μM). All experiments were performed on leaf discs of tobacco plants stably overexpressing GFP-CDC48. Results are means of data from three independent biological replicates (\pm SD), $n = 33$ for the control condition and $n = 30$ for the condition treated with cryptogin for 30 min. (t -test, $*p \leq 0.005$). Cry: cryptogin; n: number of measurements performed.

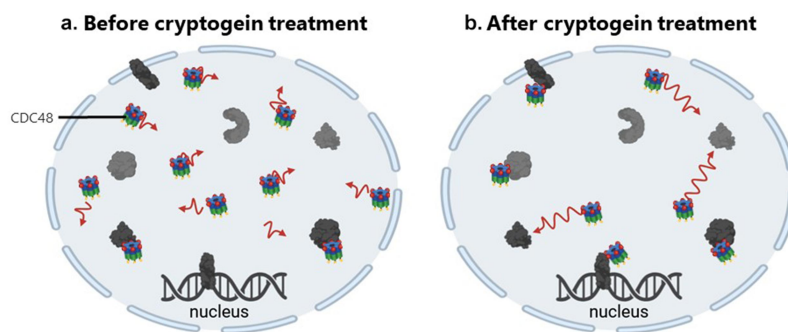


Figure 3. Schematic representation of the nuclear dynamics of CDC48 before and after cryptogei treatment. (a) Before treatment with cryptogei, nuclear CDC48 exhibits slow diffusion within the nuclei and interacts with a limited set of nuclear partners in diverse nuclear processes. (b) After cryptogei treatment, the nuclear concentration of CDC48 decreased and its diffusion increased. Additionally, CDC48 interacts more rapidly or with more nuclear partners. This enhanced mobility and interaction of CDC48 potentially contributes to the expression of defense-related genes or the maintenance of nuclear protein homeostasis. CDC48 protein partners are represented in dark gray. The length of the red arrow represents CDC48 mobility.

a decrease of the number of GFP-CDC48 molecules within the studied nuclear volumes, indicating that the cryptogei treatment leads to a reduction of the number of CDC48 molecules in the nucleus. Additionally, the association rate (K_{on}) significantly increased after cryptogei elicitation, suggesting that CDC48 interacts more rapidly and/or with more nuclear partners. However, the dissociation rate (K_{off}) remained constant in tobacco leaves regardless the treatment. So, we assume that as long as CDC48 binds to a nuclear partner, the induction of the immune response does not modify the length of the interaction with its partners. Given the increased K_{on} and unchanged K_{off} , the K_d value decreased significantly. Therefore, the affinity of CDC48 for its nuclear partners is higher after the triggering of plant defense mechanisms. CDC48 is involved in various nuclear processes, including chromatin remodeling, gene expression and INMAD.^{8,11,12} During the activation of plant defense mechanisms, a large-scale transcriptional reprogramming occurs within the nucleus.¹ In our study, after cryptogei infiltration, we measured an increase of the diffusion coefficient (D) of CDC48 in the nucleus, suggesting its nuclear remobilization after the activation of the plant immune response. Furthermore, the increase of the association rate (K_{on}) suggested that CDC48 interacts with a broader and novel set of nuclear partners, potentially contributing to the expression of defense-related genes and the maintenance of nuclear protein homeostasis, as described in processes like chromatin-associated degradation (CAD) and INMAD. The decrease of the dissociation constant (K_d) further supports that CDC48 is specifically remobilized during plant immunity and strongly engaged with its new nuclear partners. These findings provide new insights into the nuclear role of CDC48 during defense mechanisms, suggesting that CDC48 is a nuclear regulator of plant immunity (Figure 3).

Acknowledgments

We thank the facilities of the DIImaCell Imaging Center (L'Institut Agro Dijon, INRAE, INSERM, Université Bourgogne Europe, Université Marie & Louis Pasteur, Dijon, France).

Disclosure statement

No potential conflict of interest was reported by the author(s).

Funding

This work was funded by the Agence Nationale de la Recherche (grant « Algae-Nitric Oxide Synthases (ALGAE-NOS)», number 18-CE20-0022-02) and by the TRANSBIO graduate school [INTERPROT, grant number 2023Y-31560].

ORCID

Damien Inès  <http://orcid.org/0009-0000-0524-4141>

Authors' contributions

D.I. and C.R. and P.W. performed the experiments, D.I. and A. L. analyzed the data and D.I. wrote the manuscript. D.W., P-E.C. and C.R. conceived the research project, designed the experiments and edited the manuscript. D.W. and C.R. coordinate the projects listed in the funding section.

Availability of data and materials

Data are either provided in the manuscript in the main document or as supporting information or can be requested from the corresponding author.

Ethical approval

Not applicable

References

1. Padmanabhan MS, Dinesh-Kumar SP. All hands on deck—the role of chloroplasts, endoplasmic reticulum, and the nucleus in driving plant innate immunity. *MPMI*. 2010;23(11):1368–1380. doi: 10.1094/MPMI-05-10-0113.
2. Maleck K, Levine A, Eulgem T, Morgan A, Schmid J, Lawton KA, Dangl JL, Dietrich RA. The transcriptome of *Arabidopsis thaliana* during systemic acquired resistance. *Nat Genet*. 2000;26(4):403–410. doi: 10.1038/82521.
3. Garcia-Brugger A, Lamotte O, Vandelle E, Bourque S, Lecourieux D, Poinssot B, Wendehenne D, Pugin A. Early

- signaling events induced by elicitors of plant defenses. *MPMI*. 2006;19(7):711–724. doi: [10.1094/MPMI-19-0711](https://doi.org/10.1094/MPMI-19-0711).
4. Peng Y, van Wersch R, Zhang Y. Convergent and divergent signaling in PAMP-Triggered immunity and effector-triggered immunity. *MPMI*. 2018;31(4):403–409. doi: [10.1094/MPMI-06-17-0145-CR](https://doi.org/10.1094/MPMI-06-17-0145-CR).
 5. Jones JDG, Dangl JL. The plant immune system. *Nature*. 2006;444(7117):323–329. doi: [10.1038/nature05286](https://doi.org/10.1038/nature05286).
 6. Zhou B, Zeng L. Conventional and unconventional ubiquitination in plant immunity. *Mol Plant Pathol*. 2017;18(9):1313–1330. doi: [10.1111/mpp.12521](https://doi.org/10.1111/mpp.12521).
 7. Inès D, Courty P-E, Wendehenne D, Rosnoblet C. CDC48 in plants and its emerging function in plant immunity. *Trends Plant Sci*. 2024;29(7):786–798. doi: [10.1016/j.tplants.2023.12.013](https://doi.org/10.1016/j.tplants.2023.12.013).
 8. Calvanese E, Gu Y, Spoel S. Towards understanding inner nuclear membrane protein degradation in plants. *J Exp Botany*. 2022;73(8):2266–2274. doi: [10.1093/jxb/erac037](https://doi.org/10.1093/jxb/erac037).
 9. Deegan TD, Mukherjee PP, Fujisawa R, Polo Rivera C, Labib K. CMG helicase disassembly is controlled by replication fork DNA, replisome components and a ubiquitin threshold. *eLife*. 2020;9:e60371. doi: [10.7554/eLife.60371](https://doi.org/10.7554/eLife.60371).
 10. Martín-Rufo R, de la Vega-Barranco G, Lecona E. Ubiquitin and SUMO as timers during DNA replication. *Semin Cell & Dev Biol*. 2022;132:62–73. doi: [10.1016/j.semcdb.2022.02.013](https://doi.org/10.1016/j.semcdb.2022.02.013).
 11. Mérai Z, Chumak N, García-Aguilar M, Hsieh T-F, Nishimura T, Schoft VK, Bindics J, Ślusarz L, Arnoux S, Opravil S, et al. The AAA-ATPase molecular chaperone Cdc48/p97 disassembles sumoylated centromeres, decondenses heterochromatin, and activates ribosomal RNA genes. *Proc Natl Acad Sci USA*. 2014;111(45):16166–16171. doi: [10.1073/pnas.1418564111](https://doi.org/10.1073/pnas.1418564111).
 12. Ohkuni K, Gliford L, Au W-C, Suva E, Kaiser P, Basrai MA. Cdc48Ufd1/Npl4 segregase removes mislocalized centromeric histone H3 variant CENP-A from non-centromeric chromatin. *Nucleic Acids Res*. 2022;50(6):3276–3291. doi: [10.1093/nar/gkac135](https://doi.org/10.1093/nar/gkac135).
 13. Singh AN, Oehler J, Torrecilla I, Kilgas S, Li S, Vaz B, Guérillon C, Fielden J, Hernandez-Carralero E, Cabrera E, et al. The p97–ataxin 3 complex regulates homeostasis of the DNA damage response E3 ubiquitin ligase RNF8. *The EMBO J*. 2019;38(21):e102361. doi: [10.15252/emboj.2019102361](https://doi.org/10.15252/emboj.2019102361).
 14. Torrecilla I, Oehler J, Ramadan K. The role of ubiquitin-dependent segregase p97 (VCP or Cdc48) in chromatin dynamics after DNA double strand breaks. *Phil Trans R Soc B*. 2017;372(1731):20160282. doi: [10.1098/rstb.2016.0282](https://doi.org/10.1098/rstb.2016.0282).
 15. Wilcox AJ, Laney JD. A ubiquitin-selective AAA-ATPase mediates transcriptional switching by remodelling a repressor–promoter DNA complex. *Nat Cell Biol*. 2009;11(12):1481–1486. doi: [10.1038/ncb1997](https://doi.org/10.1038/ncb1997).
 16. Lehner MH, Walker J, Temcinaite K, Herlihy A, Taschner M, Berger AC, Corbett AH, Dirac Svejstrup AB, Svejstrup JQ. Yeast Smy2 and its human homologs GIGYF1 and -2 regulate Cdc48/VCP function during transcription stress. *Cell Rep*. 2022;41(4):111536. doi: [10.1016/j.celrep.2022.111536](https://doi.org/10.1016/j.celrep.2022.111536).
 17. Nakase Y, Murakami H, Suma M, Nagano K, Wakuda A, Kitagawa T, Matsumoto T. Cdc48 and its co-factor Ufd1 extract CENP-A from centromeric chromatin and can induce chromosome elimination in the fission yeast *Schizosaccharomyces pombe*. *Biol Open*. 2024;13:bio060287. doi: [10.1242/bio.060287](https://doi.org/10.1242/bio.060287).
 18. Rosnoblet C, Bègue H, Blanchard C, Pichereaux C, Besson-Bard A, Aimé S, Wendehenne D. Functional characterization of the chaperon-like protein Cdc48 in cryptogam-induced immune response in tobacco. *Plant Cell & Environ*. 2017;40(4):491–508. doi: [10.1111/pce.12686](https://doi.org/10.1111/pce.12686).
 19. Rosnoblet C, Chatelain P, Klinguer A, Bègue H, Winckler P, Pichereaux C, Wendehenne D. The chaperone-like protein Cdc48 regulates ubiquitin-proteasome system in plants. *Plant Cell & Environ*. 2021;44(8):2636–2655. doi: [10.1111/pce.14073](https://doi.org/10.1111/pce.14073).
 20. Copeland C, Woloshen V, Huang Y, Li X. AtCDC48A is involved in the turnover of an NLR immune receptor. *The Plant J*. 2016;88(2):294–305. doi: [10.1111/tpj.13251](https://doi.org/10.1111/tpj.13251).
 21. Nicolas-Francis V, Besson-Bard A, Meschini S, Klinguer A, Bonnotte A, Héloir M-C, Citerne S, Inès D, Hichami S, Wendehenne D, et al. CDC48 regulates immunity pathway in tobacco plants. *Plant Physiol & Biochem*. 2024;211:108714. doi: [10.1016/j.plaphy.2024.108714](https://doi.org/10.1016/j.plaphy.2024.108714).
 22. Bonnet P, Bourdon E, Ponchet M, Blein J-P, Ricci P. Acquired resistance triggered by elicitors in tobacco and other plants. *Eur J Plant Pathol*. 1996;102(2):181–192. doi: [10.1007/BF01877105](https://doi.org/10.1007/BF01877105).
 23. Wahl M, Gregor I, Patting M, Enderlein J. Fast calculation of fluorescence correlation data with asynchronous time-correlated single-photon counting. *Opt Express*. 2003;11(26):3583–3591. doi: [10.1364/OE.11.003583](https://doi.org/10.1364/OE.11.003583).
 24. Enderlein J, Gregor I. Using fluorescence lifetime for discriminating detector afterpulsing in fluorescence-correlation spectroscopy. *Rev Sci Instruments*. 2005;76(3):033102. doi: [10.1063/1.1863399](https://doi.org/10.1063/1.1863399).
 25. Michelman-Ribeiro A, Mazza D, Rosales T, Stasevich TJ, Boukari H, Rishi V, Vinson C, Knutson JR, McNally JG. Direct measurement of association and dissociation rates of DNA binding in live cells by fluorescence correlation spectroscopy. *Biophys J*. 2009;97(1):337–346. doi: [10.1016/j.bpj.2009.04.027](https://doi.org/10.1016/j.bpj.2009.04.027).
 26. Dertinger T, Pacheco V, von der Hocht I, Hartmann R, Gregor I, Enderlein J. Two-focus fluorescence correlation spectroscopy: a new tool for accurate and absolute diffusion measurements. *ChemPhysChem*. 2007;8(3):433–443. doi: [10.1002/cphc.200600638](https://doi.org/10.1002/cphc.200600638).
 27. Aker J, Hesselink R, Engel R, Karlova R, Borst JW, Visser AJWG, de Vries SC. In vivo hexamerization and characterization of the Arabidopsis AAA ATPase CDC48A complex using Förster resonance energy transfer-fluorescence lifetime imaging microscopy and fluorescence correlation spectroscopy. *Plant Physiol*. 2007;145(2):339–350. doi: [10.1104/pp.107.103986](https://doi.org/10.1104/pp.107.103986).
 28. Duan W, Li K, Li J, Ding N, Wang S, Zou Y, Zhang Z, Duan Z, Xing J. Exploring membrane proteins dynamic in plant cells with fluorescence correlation spectroscopy. *New Crops*. 2025;2:100032. doi: [10.1016/j.ncrops.2024.100032](https://doi.org/10.1016/j.ncrops.2024.100032).
 29. Li X, Wang X, Yang Y, Li R, He Q, Fang X, Luu D-T, Maurel C, Lin J. Single-molecule analysis of PIP2₁ dynamics and partitioning reveals multiple modes of Arabidopsis plasma membrane Aquaporin Regulation[C][W]. *Plant Cell*. 2011;23(10):3780–3797. doi: [10.1105/tpc.111.091454](https://doi.org/10.1105/tpc.111.091454).